

Electronic Supplementary Information (ESI) for

Three-stage pH-Switchable Organic Chromophores with Large Nonlinear Optical Responses and Switching Contrasts

Stein van Bezouw,^{§,a} Min-Jeong Koo,^{§,b} Seung-Chul Lee,^b Seung-Heon Lee,^b Jochen Campo,^a

O-Pil Kwon,^{*,b} and Wim Wenseleers^{*,a}

^aDepartment of Physics, University of Antwerp, Campus Drie Eiken (CDE), Universiteitsplein 1, B-2610 Wilrijk, Belgium.

^bDepartment of Molecular Science and Technology, Ajou University, Suwon 443-749, Korea.

E-mail: opilkwon@ajou.ac.kr

E-mail: Wim.Wenseleers@uantwerpen.be

[§]These authors contributed equally to this work.

Table of contents

- A. Synthesis of the chromophores
- B. pH-dependent absorption and fluorescence measurements
- C. Fluorescence quantum yield measurements
- D. Measurements of pK_a values
- E. Hyper-Rayleigh scattering measurements
- F. Summary table of linear and nonlinear optical properties
- G. Solvatochromism of HM-NHQ St2
- H. Solvatochromism of OH-NHQ St2

A. Synthesis of the chromophores

As shown in Fig. S1, three ionic π -conjugated compounds (DA-NHQ-T, HM-NHQ-T and OH-NHQ-T) consist of quinolinium cations (DA-NHQ (2-(4-(dimethylamino)styryl)quinolinium), HM-NHQ (2-(4-hydroxy-3-methoxystyryl)quinolinium) and OH-NHQ (2-(4-hydroxystyryl)quinolinium), respectively) with 4-methylbenzenesulfonate (T) counter anion. All quinolinium compounds are synthesized by a Knoevenagel condensation of the intermediate 2-methylquinolinium 4-methylbenzenesulfonate (NHQ-T) and the corresponding benzaldehyde including a pH-sensitive electron-donating group (EDG).

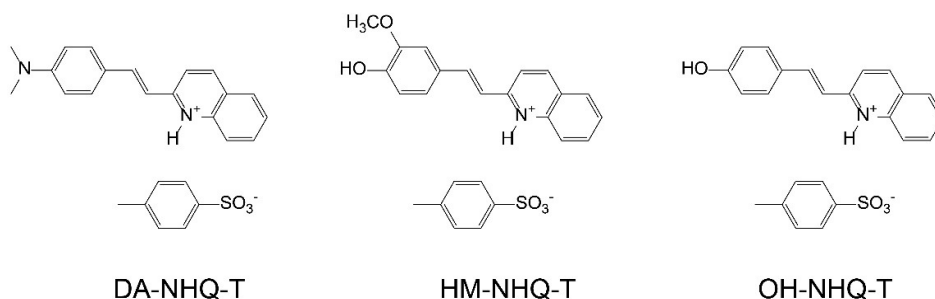


Fig. S1. Chemical structure of investigated ionic π -conjugated quinolinium chromophores.

A.1 Synthesis of intermediates

2-Methylquinolinium 4-methylbenzenesulfonate (NHQ-T): 2-Methylquinoline (1.96 mL, 13.8 mmol) and 4-methylbenzenesulfonic acid (2.69 g, 13.8 mmol) were dissolved in 1,2-dimethoxyethane (15 mL) and stirred at 50 °C for 5.5 hours. The white precipitated powder was filtered and purified by recrystallization in methanol. Yield = 13 %. ¹H-NMR (400 MHz, DMSO-d₆, δ): 9.04 (d, 1H, J = 8.4, C₅H₃N), 8.31 (d, 1H, J = 8.0, C₆H₄), 8.19 (d, 1H, J = 8.4, C₅H₃N), 8.11 (t, 1H, J = 7.6, C₆H₄), 7.97 (d, 1H, J = 8.8, C₆H₄), 7.90 (t, 1H, J = 7.4, C₆H₄), 7.49 (d, 2H, J = 8.0, C₆H₄SO₃⁻), 7.10 (d, 2H, J = 8.0, C₆H₄SO₃⁻), 2.94 (s, 3H, CH₃), 2.28 (s, 3H, CH₃). Elemental analysis for C₁₇H₁₇NO₃S: Calcd. C 64.74, H 5.43, N 4.44, S 10.17; Found: C 64.76, H 5.40, N 4.46, S 10.09.

A.2 Synthesis of quinolinium chromophores

2-(4-(Dimethylamino)styryl)quinolinium 4-methylbenzenesulfonate (DA-NHQ-T): DA-NHQ-T compound was synthesized by a Knoevenagel condensation. NHQ-T (2 g, 6.34 mmol) and 4-(dimethylamino)benzaldehyde (0.965 g, 6.34 mmol) were dissolved in ethanol (20 mL) in the presence of piperidine catalyst (125 μ L, 1.27 mmol, 0.2 equiv.). The solution was stirred at 70 °C for 4 days. After cooling to room temperature, a brown crystalline powder precipitated. The brown powder was filtered and purified by recrystallization in methanol. Yield = 28 %. ¹H-NMR (400 MHz, DMSO-d₆, δ): 15.01 (s, 1H, C₅H₃N), 8.81 (d, 1H, J = 9.2, C₅H₃N), 8.33 (d, 1H, J = 9.2, C₆H₄), 8.22 (d, 1H, J = 16, CH), 8.16 (d, 1H, J = 8.4, C₆H₄), 8.05 (d, 1H, J = 8.0, C₅H₃N), 7.99 (t, 1H, J = 7.8, C₆H₄), 7.76 (t, 1H, J = 7.6, C₆H₄), 7.64 (d, 2H, J = 8.8, C₆H₄SO₃⁻), 7.48 (d, 1H, J = 8.0, C₆H₄), 7.22 (d, 1H, J = 16, CH), 7.11 (d, 2H, J = 8.0, C₆H₄SO₃⁻), 6.84 (d, 2H, J = 8.8, C₆H₄), 3.06 (s, 6H, N(CH₃)₂), 2.29 (s, 3H, CH₃). Elemental analysis for C₂₆H₂₆N₂O₃S·H₂O: Calcd. C 67.22, H 6.07, N 6.03, S 6.90; Found: C 67.51, H 5.94, N 6.12, S 6.85.

2-(4-Hydroxy-3-methoxystyryl)quinolinium 4-methylbenzenesulfonate (HM-NHQ-T): HM-NHQ-T compound was synthesized by a Knoevenagel condensation, in a similar manner as DA-NHQ-T. NHQ-T (2 g, 6.34 mmol) and 4-hydroxy-3-methoxybenzaldehyde (0.975 g, 6.34 mmol) were dissolved in ethanol (20 mL) in the presence of piperidine catalyst (125 μ L, 1.27 mmol, 0.2 equiv.). The solution was stirred at 70 °C for 40 hours. After cooling to room temperature, a precipitated orange powder was filtered and purified by recrystallization in methanol. Yield = 47 %. ¹H-NMR (400 MHz, DMSO-d₆, δ): 8.89 (d, 1H, J = 8.4, C₅H₃N), 8.35 (d, 1H, J = 8.8, C₆H₄), 8.19 (d, 1H, J = 16, CH), 8.18 (d, 1H, J = 8.4, C₆H₄), 8.11 (d, 1H, J = 8.8, C₅H₃N), 8.02 (t, 1H, J = 7.8, C₆H₄), 7.80 (t, 1H, J = 7.4, C₆H₄), 7.48 (d, 2H, J = 8.0, C₆H₄SO₃⁻), 7.38 (d, 1H, J = 16, CH), 7.37 (s, 1H, C₆H₃), 7.24 (d, 1H, J = 8.0, C₆H₃), 7.11 (d, 2H, J = 7.6, C₆H₄SO₃⁻), 6.92 (d, 1H, J = 8.0, C₆H₃), 3.88 (s, 3H, OCH₃), 2.28 (s, 3H, CH₃). Elemental analysis for C₂₅H₂₃NO₅S: Calcd. C 66.80, H 5.16, N 3.12, S 7.13; Found: C 66.71, H 5.12, N 3.12, S 7.14.

2-(4-Hydroxystyryl)quinolinium 4-methylbenzenesulfonate (OH-NHQ-T): OM-NHQ-T compound was synthesized by a Knoevenagel condensation, in a similar manner as DA-NHQ-T. NHQ-T (2 g, 6.34 mmol) and 4-hydroxybenzaldehyde (0.790 g, 6.34 mmol) were dissolved in ethanol (20 mL) in the presence of piperidine catalyst (125 μ l, 1.27 mmol, 0.2 equiv.). The solution was stirred at 70 °C for 41 hours. After cooling to room temperature, a precipitated orange powder was filtered and purified by recrystallization in methanol. Yield = 55 %. $^1\text{H-NMR}$ (400 MHz, DMSO- d_6 , δ): 8.93 (d, 1H, J = 8.8, $\text{C}_5\text{H}_3\text{N}$), 8.40 (d, 1H, J = 8.8, C_6H_4), 8.23 (d, 1H, J = 15.2, CH), 8.22 (d, 1H, J = 8.8, C_6H_4), 8.13 (d, 1H, J = 8.4, $\text{C}_5\text{H}_3\text{N}$), 8.04 (t, 1H, J = 7.6, C_6H_4), 7.82 (t, 1H, J = 7.4, C_6H_4), 7.65 (d, 2H, J = 8.8, $\text{C}_6\text{H}_4\text{SO}_3^-$), 7.50 (d, 2H, J = 8.4, $\text{C}_6\text{H}_4\text{SO}_3^-$), 7.34 (d, 1H, J = 16.4, CH), 7.11 (d, 2H, J = 8.0, C_6H_4), 6.92 (d, 2H, J = 8.4, C_6H_4), 2.28 (s, 3H, CH_3). Elemental analysis for $\text{C}_{24}\text{H}_{21}\text{NO}_4\text{S}$: Calcd. C 68.72, H 5.05, N 3.34, S 7.64; Found: C 68.71, H 5.04, N 3.38, S 7.60.

B. pH-dependent absorption and fluorescence measurements

The pH of solutions of DA-NHQ-T, HM-NHQ-T, and OH-NHQ-T in methanol were controlled by adding diluted solutions in methanol of 50% NaOH in water, and 37% HCl in water, so that the amount of water in the dye solutions remains limited – except for the DA-NHQ-T, for which larger quantities of 37% HCl in water were needed to reach St1. The pH of solutions of DA-NHQ-T, HM-NHQ-T, and OH-NHQ-T in water were controlled by adding mother solutions: 4 M HCl in dioxane, 5×10^{-2} M NaOH in methanol, and 15 M NaOH in water. The pH values of the solutions in methanol were measured using a Lab 850 glass electrode pH meter from Schott Instruments, and a Metrohm model 780 pH meter was used for the solutions in water. The UV-vis absorption spectra of the solutions in methanol were recorded on a Varian Cary 5E absorption spectrometer, while those in water were recorded on a Jasco V-670 absorption spectrometer, in both cases using a quartz cuvette with 10mm path-length. Fluorescence spectra were recorded by a custom-built fluorescence spectrometer system based on an Ocean Optics Maya 2000 pro spectrometer at an excitation wavelength of 385 nm (Ergonomic LED Light Sources LLS-385).

B.1. pH-dependent absorption and fluorescence measurements in methanol

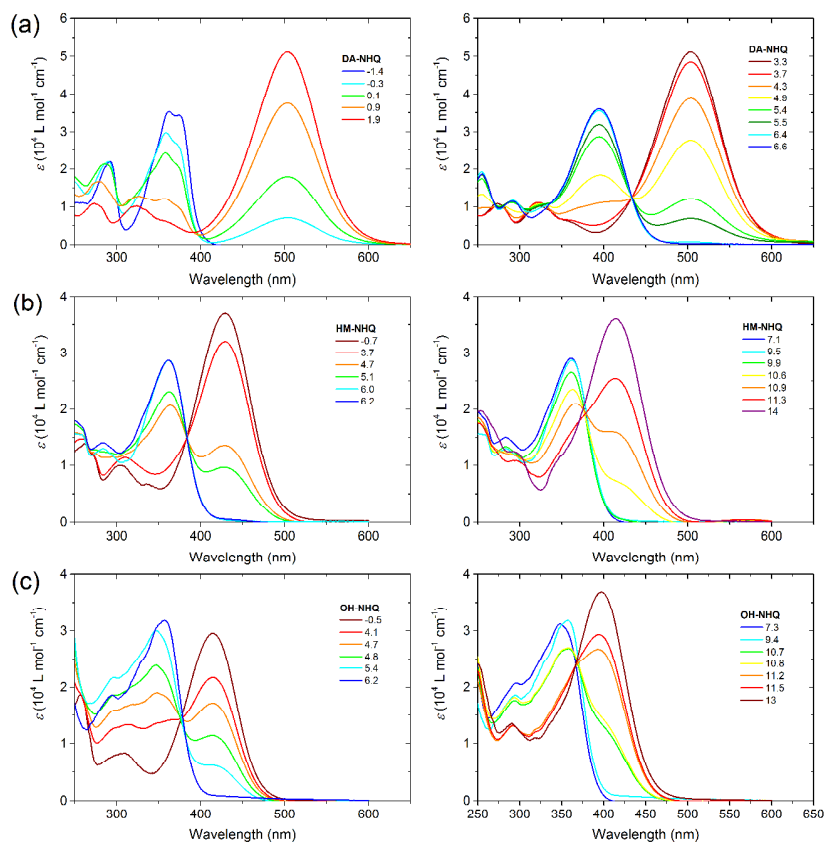


Fig. S2. Absorption spectra of (a) DA-NHQ-T, (b) HM-NHQ-T and (c) OH-NHQ-T in methanol solution as a function of pH, corresponding to the 2D data shown in Fig. 2a.

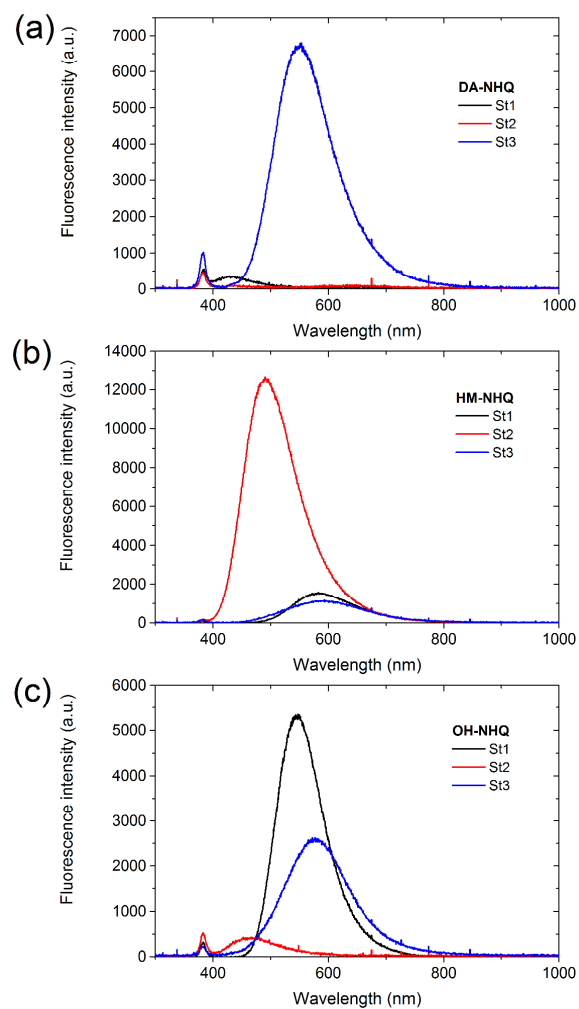


Fig. S3. Fluorescence spectra of the three stages of (a) DA-NHQ-T, (b) HM-NHQ-T and (c) OH-NHQ-T in methanol solution. These spectra are used to interpolate the spectra at other pH values using the Henderson-Hasselbalch equation, yielding the 2D data shown in Fig. 2b.

B.2. pH-dependent absorption and fluorescence measurements in water

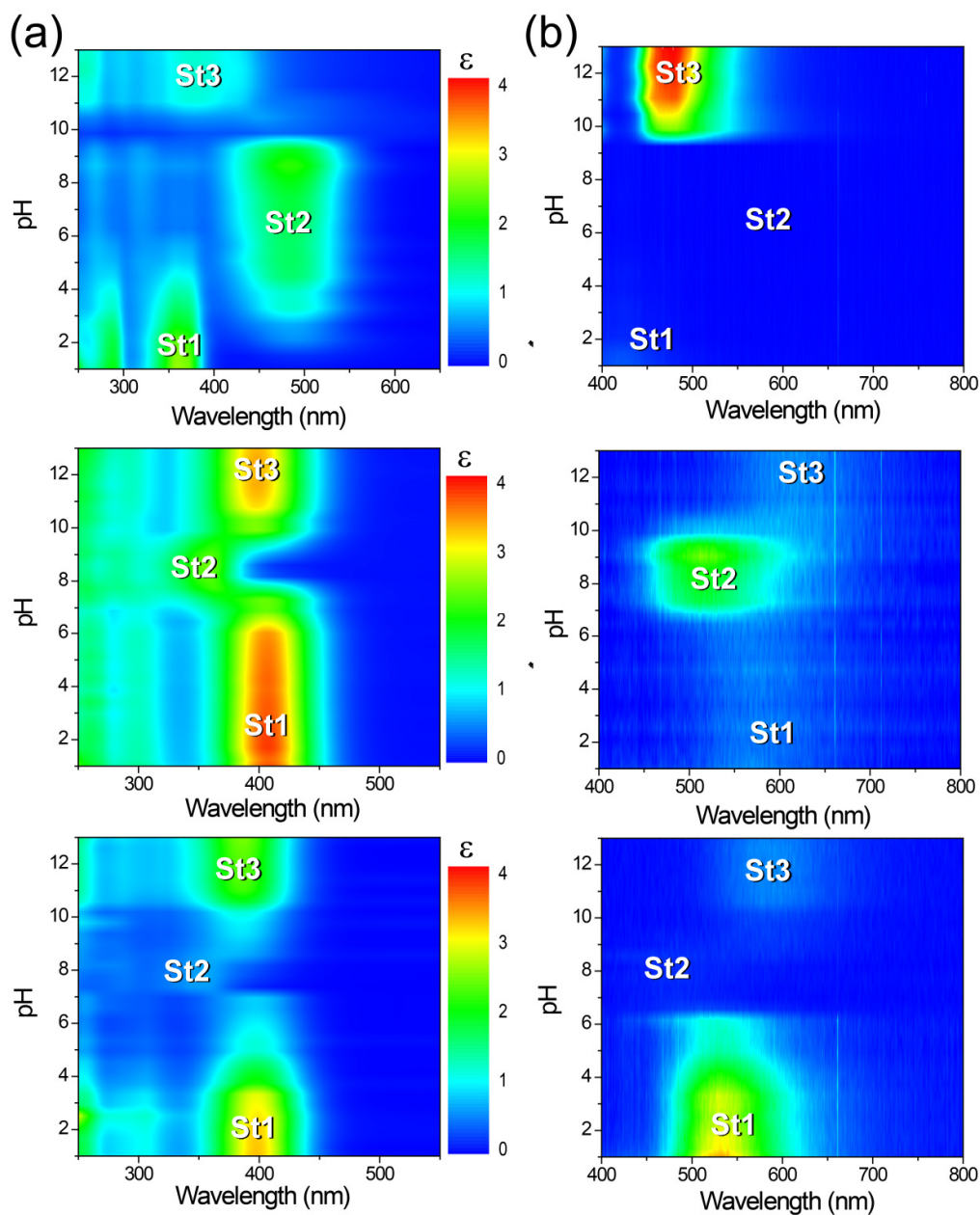


Fig. S4. (a) Absorption (extinction coefficient ϵ in $10^4 \text{ M}^{-1} \text{ cm}^{-1}$) and (b) fluorescence contour plots of DA-NHQ (top), HM-NHQ (middle) and OH-NHQ (bottom) in aqueous solution as a function of pH (see details in Fig. S5 and S6).

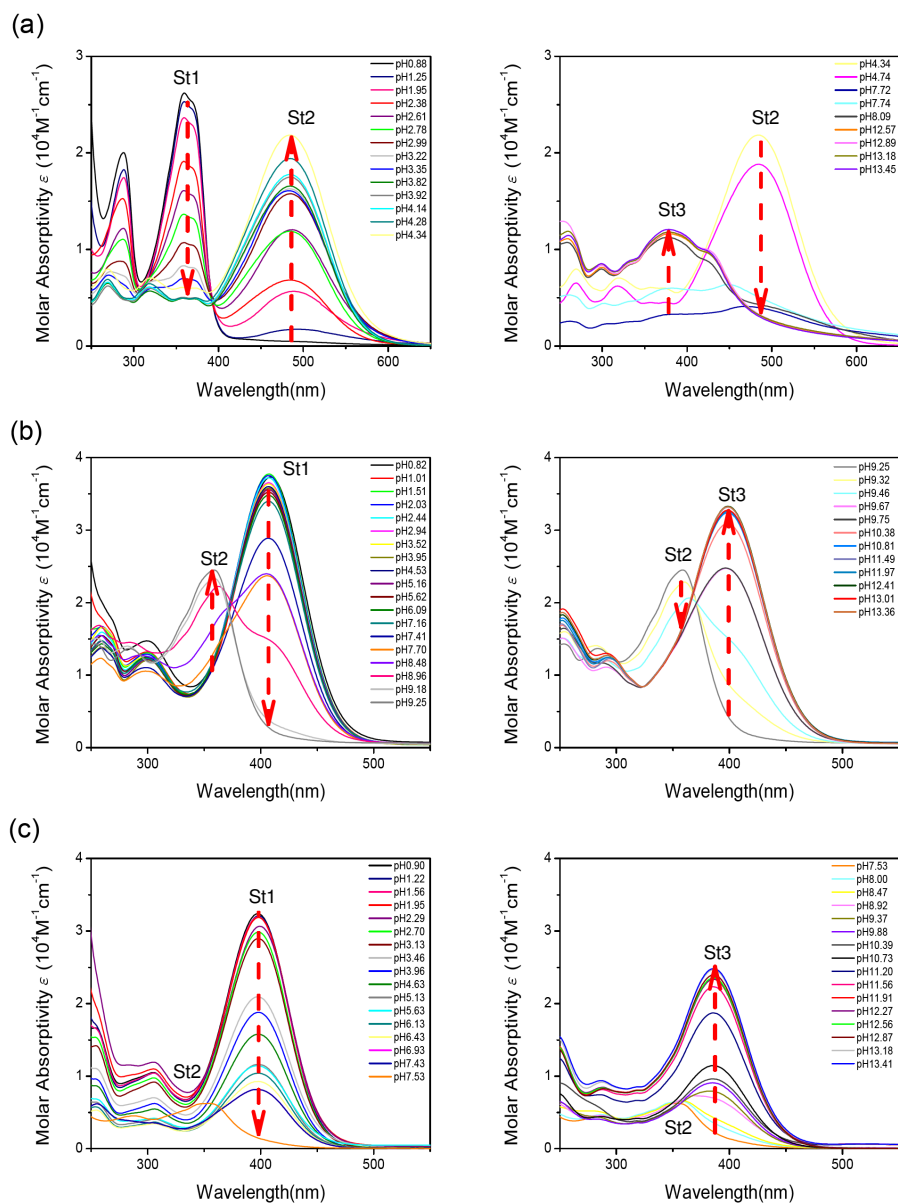


Fig. S5. Absorption spectra of (a) DA-NHQ-T, (b) HM-NHQ-T and (c) OH-NHQ-T in aqueous solution as a function of pH, corresponding to the 2D data shown in Fig. S4a.

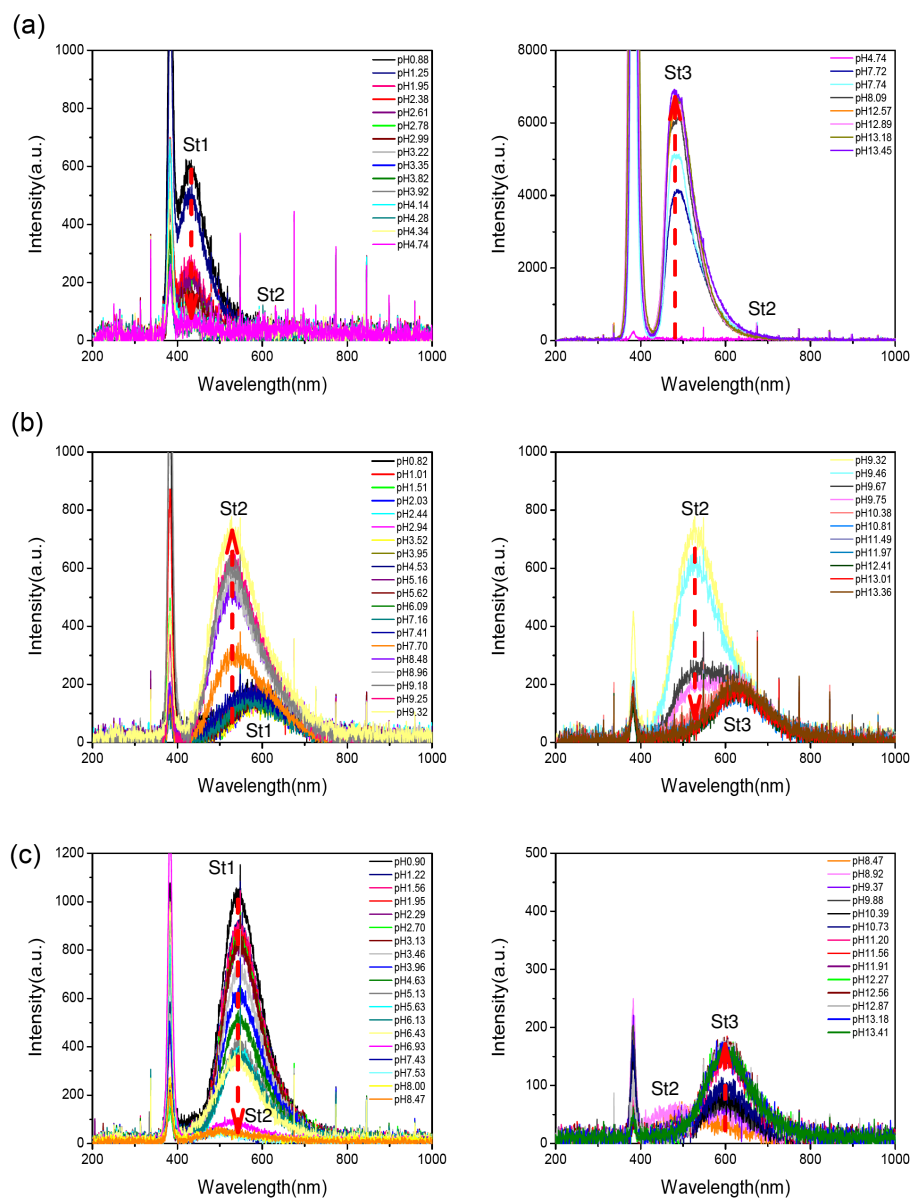


Fig. S6. Fluorescence spectra of (a) DA-NHQ-T, (b) HM-NHQ-T and (c) OH-NHQ-T in aqueous solution as a function of pH, corresponding to the 2D data shown in Fig. S4b.

C. Fluorescence quantum yield measurements

Fluorescence quantum yields, Φ , were measured in methanol solution, according to the literature.¹ Coumarin-153 with $\Phi = 45\%$ in methanol was used as a reference. The excitation wavelength (λ_{exc}) of the quinolinium compounds and the reference was identical.

Table S1. Fluorescence quantum yield Φ in methanol solution.

	DA- NHQ	HM-NHQ	OH-NHQ
St1	0.24% at pH = -1.57 with $\lambda_{\text{exc}} = 385$ nm	0.49% at pH = -1.53 with $\lambda_{\text{exc}} = 385$ nm	2.45% at pH = 0.0 with $\lambda_{\text{exc}} = 385$ nm
St2	0.36% at pH = 1.75 with $\lambda_{\text{exc}} = 470$ nm	2.22% at pH = 7.53 with $\lambda_{\text{exc}} = 385$ nm	0.43% at pH = 6.95 with $\lambda_{\text{exc}} = 365$ nm
St3	3.15% at pH = 8.38 with $\lambda_{\text{exc}} = 385$ nm	0.60% at pH = 11.13 with $\lambda_{\text{exc}} = 385$ nm	1.26% at pH = 11.5 with $\lambda_{\text{exc}} = 385$ nm

D. Measurements of pK_a values

The pK_a values of the chromophores (DA-NHQ-T, HM-NHQ-T, OH-NHQ-T) and intermediates (phenolic electron-donating 4-hydroxy-3-methoxybenzaldehyde, quinolinium electron-withdrawing NHQ-T) were determined in methanol solution by using a rearranged Henderson-Hasselbalch equation reported in literature.²

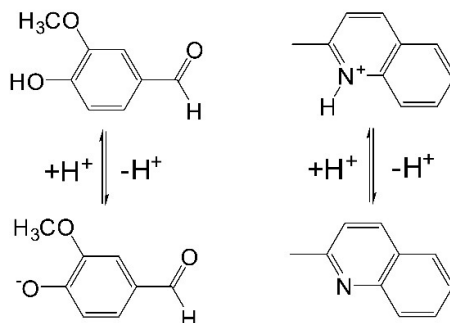


Fig. S7. Chemical structure of 4-hydroxy-3-methoxybenzaldehyde (EDG) and NHQ-T (EWG) of HM-NHQ-T in acidic and basic conditions

Phenolic EDG and Quinolinium EWG: The pK_a value of the phenolic group of electron-donating 4-hydroxy-3-methoxybenzaldehyde is 8.33 in methanol, which also agrees well with literature (pK_a = 8.33 in water).³ In addition, analogous phenolic group of 2-(4-hydroxy-3-methoxystyryl)quinolinium, 2-(4-hydroxystyryl)quinolinium 2-(4-hydroxy-3-methoxystyryl)pyridinium and 2-(4-hydroxystyryl)pyridinium derivatives exhibit similar range of pK_a values (7.9 – 8.51 in water).⁴ The pK_a value of quinolinium group of electron-withdrawing 2-methylquinolinium 4-methylbenzenesulfonate (NHQ-T) is pK_a = 2.85 in methanol.

Three-stage chromophores: The pK_a values of DA-NHQ cations of DA-NHQ-T are pK_{a,1} = 0.4 for the dimethylamino group and pK_{a,2} = 4.8 for the quinolinium group. The pK_a values of HM-NHQ cations of HM-NHQ-T are pK_{a,1} = 4.5 for the phenolic group and pK_{a,2} = 11.0 for the quinolinium group. The pK_a values of OH-NHQ cations of OH-NHQ-T are pK_{a,1} = 4.5 for the phenolic group and pK_{a,2} = 10.9 for the quinolinium group.

E. Hyper-Rayleigh scattering (HRS) measurements

The compounds were dissolved in methanol (Acros, 99.9%, for residue analysis) and the pH was tuned by adding small amounts of 37mass% HCl (Merck, for analysis, in water) and 50mass% NaOH (Acros, for analysis, in water). The SO NLO responses (hyperpolarizability β) of the various stages of the compounds were determined using the highly sensitive and wavelength tunable hyper-Rayleigh setup described before.⁵ In short, a Ti:sapphire chirped-pulse regenerative laser amplifier (Spectra-Physics Spitfire) pumps an automatically tunable optical parametric amplifier (Light Conversion TOPAS-800-ps) to provide 2ps pulses at a 1kHz repetition rate with a continuously tunable wavelength. The output beam is focused into a cuvette containing the solution under investigation, and the generated HRS light is detected using a spectrograph, coupled to a nitrogen-cooled CCD, that ensures parallel detection of a narrow spectral range around the second harmonic wavelength. This spectral analysis is essential for systematic and complete subtraction of any multi-photon fluorescence contributions that often occur, and are easily distinguished as a broad background. All β values are determined by reliable calibration against the HRS signal of the pure solvent itself, which we extensively calibrated before against CHCl_3 .⁵ Values are given as the β_{zzz} -component, making the usual assumption that this is the only significant β tensor component (in general a very good approximation for elongated push-pull compounds such as those considered here), in which case $\beta_{\text{HRS}} = (6/35)^{1/2} \beta_{zzz}$.

Both on and off resonance β values were measured, and these were extrapolated to zero frequency values using a β dispersion model developed before in our group incorporating both homogeneous and inhomogeneous broadening (HIV model).⁶ The only shape-determining fit parameter in this model, *i.e.* the amount of inhomogeneous broadening G_{inhom} , was optimized to the HRS data for the various stages of the compounds, yielding for HM-NHQ: St1: 1159 cm^{-1} , St2: 0 cm^{-1} (*i.e.* the homogeneous limit gives the best fit), St3: 1608 cm^{-1} ; for OH-NHQ: St1: 461 cm^{-1} , St2: 0 cm^{-1} (*i.e.* the homogeneous limit gives the best fit), St3: 1523 cm^{-1} ; and for DA-NHQ: St1: 566 cm^{-1} , St2: 1359 cm^{-1} ,

St3: 1656cm^{-1} . While error bars on G_{inhom} are large, in general the use of this intermediate model gives significant improvement over the purely homogeneous/inhomogeneous cases (except for HM-NHQ St2 and OH-NHQ St2, where the best fit is obtained for the homogeneous limiting case).

Methanol was chosen as a solvent and internal reference standard because of the high solubility for all stages of the compounds, its protic nature, and complete miscibility with water. Deuterated methanol (VWR Chemicals, $<0.03\%$ water, 99.8% atom% deuterium) was used for its extended IR transparency, to allow for measurements at longer laser wavelengths. Deuterated methanol was found to have the same β as the nondeuterated form within experimental errors, in agreement with previous investigations by Kaatz and Shelton.⁷ The amount of H_2O introduced by adding the required quantities of the $50\text{mass}\%$ NaOH and $37\text{mass}\%$ HCl stock solutions was low in most cases ($<0.1\%$), insignificantly influencing the polarity of the solution. To reach DA-NHQ St1, however, that has a very low pK_a value, $33\text{volume}\%$ of the final solution was $37\text{mass}\%$ HCl, so that the methanol solution contained $\sim 21\text{volume}\%$ H_2O in total. As this is a significant change to the environment of DA-NHQ and thus might influence its hyperpolarizability, as an additional check, DA-NHQ St2 and DA-NHQ St3 were measured at a fundamental wavelength of 1060nm in $23\text{volume}\%$ H_2O / $77\text{volume}\%$ MeOH solutions, *i.e.* at the same water/methanol ratio as for the $33\text{volume}\%[37\text{mass}\% \text{HCl}/\text{H}_2\text{O}]/67\text{volume}\%$ MeOH mixture (noting that $\sim 10\text{volume}\%$ of the latter mixture is HCl), and were found not to change significantly (see below): To calculate the effective (average) first hyperpolarizability β_{eff} of these binary solvent mixtures to be able to use them for internal calibration, the mixtures were calibrated against pure methanol (both for the $33\text{volume}\%[37\text{mass}\% \text{HCl}/\text{H}_2\text{O}] / 67\text{volume}\%$ MeOH, and the $21\text{volume}\%$ H_2O / $79\text{volume}\%$ MeOH mixtures). The refractive indices and the molarity needed for the external calibration method were calculated by linear interpolation from the values for pure methanol and water⁵ for the measurements of DA-NHQ St2 and DA-NHQ St3, and methanol and $37\text{mass}\%\text{HCl}/\text{H}_2\text{O}$ ⁸ for the measurements of DA-NHQ St1. The calculated β_{eff} for both mixtures are found to be the same within experimental error ($0.223 \times 10^{-30}\text{esu}$ and

0.216×10^{-30} esu for the MeOH/H₂O and MeOH/H₂O/HCl mixtures respectively), and are also equivalent to the β_{eff} as calculated using the formula for a binary mixture (0.229×10^{-30} esu in both cases):

$$\beta_{\text{eff,mixture}} = \sqrt{\frac{N_{\text{MeOH}}|\beta_{\text{MeOH}}|^2 + N_{\text{H}_2\text{O}}|\beta_{\text{H}_2\text{O}}|^2}{N_{\text{MeOH}} + N_{\text{H}_2\text{O}}}}$$

with β_{MeOH} ($\beta_{\text{H}_2\text{O}}$) the first hyperpolarizabilities of the two components in the mixture, *i.e.* MeOH and H₂O (for simplicity, in the three-component MeOH/H₂O/HCl system, the HRS contribution of HCl was neglected, considering HCl only as a diluent for the other two components), and N_{MeOH} ($N_{\text{H}_2\text{O}}$) their respective concentrations, supporting the assumptions made. The results for DA-NHQ St2 and DA-NHQ St3 were not influenced significantly by the addition of water compared to the measurements in pure methanol (see Table S2), indicating that this addition of water likely also does not have a significant effect on the hyperpolarizability of DA-NHQ St1.

Table S2. Comparison of experimental β values measured at 1060nm for DA-NHQ in stages St2 and St3, in pure methanol and the MeOH/H₂O binary mixture.

Solvent	Stage DA-NHQ	β (10^{-30} esu)
MeOH	St2	3577 \pm 358
	St3	243 \pm 12
79%MeOH/21%H ₂ O	St2	3422 \pm 171
	St3	235 \pm 12

F. Summary table of linear and nonlinear optical properties

Table S3. Summary of linear and nonlinear optical properties.

	DA- NHQ	HM-NHQ	OH-NHQ
wavelength of absorption maximum λ_{abs} of St1, St2, and St3 (nm) ^a	360, 505, 393	428, 362, 414	414, 345, 397
pKa (St1-to-St2, St2-to-St3) ^a	0.4, 4.8	4.5, 11.0	4.5, 10.9
wavelength of emission maximum λ_{em} of St1, St2, and St3 (nm) ^{a,b}	430, 650, 550	575, 490, 595	545, 465, 577
fluorescence switching modes (St1-St2-St3) ^{a,b}	OFF-OFF-ON	OFF-ON-OFF	ON-OFF-ON
fluorescent contrast at maximum fluorescent intensity ^{a,b}	$I_{\text{St1}}/I_{\text{St2}}=7.7$ $I_{\text{St3}}/I_{\text{St2}}=3.6$	$I_{\text{St2}}/I_{\text{St1}}=2.9$ $I_{\text{St2}}/I_{\text{St3}}=4.2$	$I_{\text{St1}}/I_{\text{St2}}=38.2$ $I_{\text{St3}}/I_{\text{St2}}=8.3$
quantum yield Φ of St1, St2, and St3 ^{a,c}	0.24%, 0.36%, 3.15%	0.49%, 2.22%, 0.60%	2.45%, 0.43%, 1.26%
β_0 of St1, St2, and St3 ($\times 10^{-30}$ esu)	31, 263, 92	98, 39, 96	75, 35, 77
β_0 switching modes (St1-St2-St3)	OFF-ON-ON	ON-OFF-ON	ON-OFF-ON
β_0 contrast	$\beta_{0,\text{St2}}/\beta_{0,\text{St1}}=9.1$ $\beta_{0,\text{St2}}/\beta_{0,\text{St3}}=2.9$	$\beta_{0,\text{St1}}/\beta_{0,\text{St2}}=2.5$ $\beta_{0,\text{St3}}/\beta_{0,\text{St2}}=2.4$	$\beta_{0,\text{St1}}/\beta_{0,\text{St2}}=2.1$ $\beta_{0,\text{St3}}/\beta_{0,\text{St2}}=2.2$
maximum β_{max} of St1, St2, and St3 ($\times 10^{-30}$ esu)	$\beta_{\text{max},\text{St1}}=507$ (764 nm) $\beta_{\text{max},\text{St2}}=3723$ (1036 nm) $\beta_{\text{max},\text{St3}}=1298$ (812 nm)	$\beta_{\text{max},\text{St1}}=1264$ (880 nm) $\beta_{\text{max},\text{St2}}=574$ (736 nm) $\beta_{\text{max},\text{St3}}=1295$ (860 nm)	$\beta_{\text{max},\text{St1}}=926$ (844 nm) $\beta_{\text{max},\text{St2}}=479$ (732 nm) $\beta_{\text{max},\text{St3}}=1127$ (820 nm)
maximum β_{max} contrast ratio	$(\beta_{\text{St2}}/\beta_{\text{St1}})_{\text{max}}=60.7$ (1056 nm) $(\beta_{\text{St2}}/\beta_{\text{St3}})_{\text{max}}=14.4$ (1072 nm)	$(\beta_{\text{St1}}/\beta_{\text{St2}})_{\text{max}}=9.27$ (916 nm) $(\beta_{\text{St3}}/\beta_{\text{St2}})_{\text{max}}=8.63$ (904 nm)	$(\beta_{\text{St1}}/\beta_{\text{St2}})_{\text{max}}=7.04$ (884 nm) $(\beta_{\text{St3}}/\beta_{\text{St2}})_{\text{max}}=7.37$ (864 nm)

^a in methanol, ^b excited at 385 nm, ^c see Table S1.

G. Solvatochromism of HM-NHQ St2

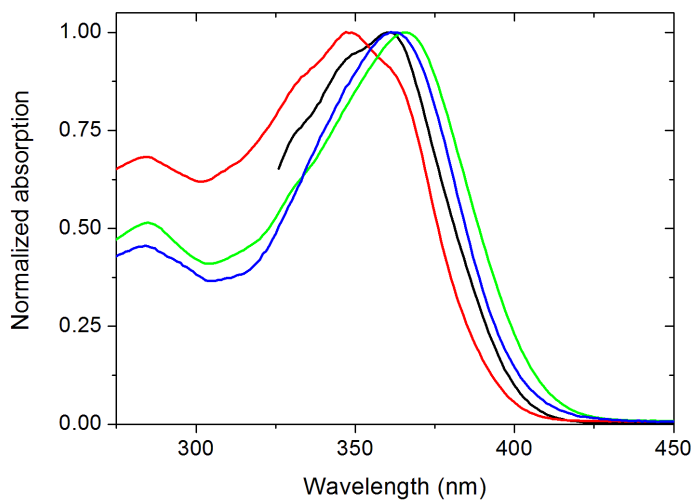


Fig. S8. Absorption spectra of HM-NHQ St2 in chloroform (red), acetone (black), dimethylformamide (green) and methanol (blue) solutions, used to determine the solvatochromism of this stage (inset in top panel of Fig. 3b). For clarity, the spectrum in acetone is shown only down to the UV absorption cut-off of acetone at around 300nm.

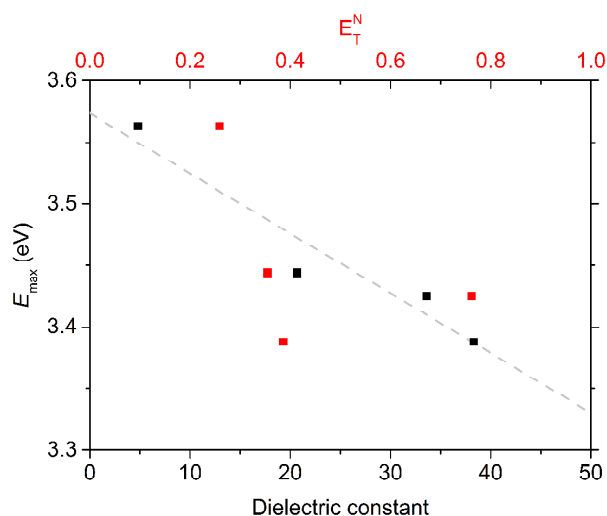


Fig. S9. Positive solvatochromism of HM-NHQ St2: lowest transition energy as a function of dielectric constant (bottom axis; black circles), Reichardt's E_T^N scale (top axis; red squares).⁹ The grey dashed line is a linear fit to the black data points serving as a guide-to-the-eye.

H. Solvatochromism of OH-NHQ St2

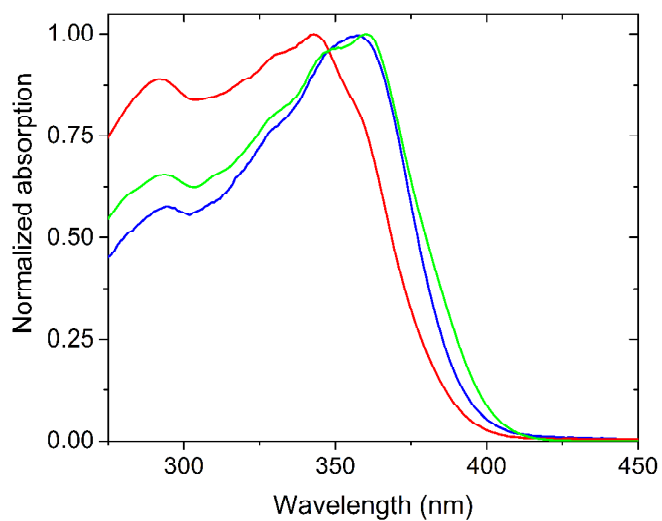


Fig. S10. Absorption spectra of OH-NHQ St2 in chloroform (red), dimethylformamide (green) and methanol (blue) solutions, used to determine the solvatochromism of this stage (inset in top panel of Fig. 3c).

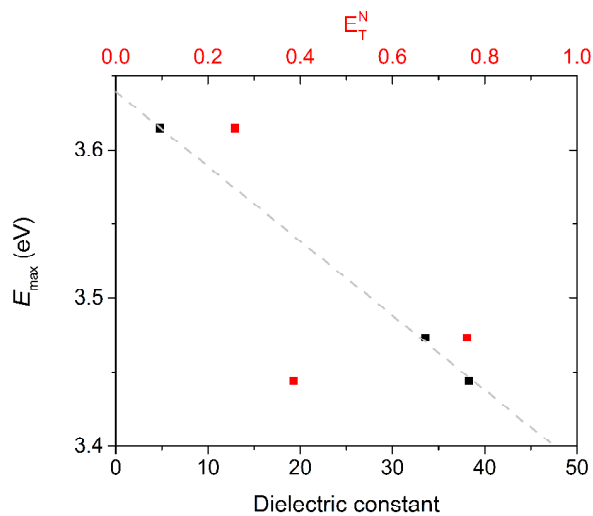


Fig. S11. Positive solvatochromism of OH-NHQ St2: lowest transition energy as a function of dielectric constant (bottom axis; black circles), Reichardt's E_T^N scale (top axis; red squares).⁹ The grey dashed line is a linear fit to the black data points serving as a guide-to-the-eye.

References

1. A. Bourdolle, M. Allali, A. D'Aleo, P. L. Baldeck, K. Kamada, J. A. G. Williams, H. Le Bozec, C. Andraud and O. Maury, *Chemphyschem*, 2013, **14**, 3361-3367.
2. Y. I. Park, O. Postupna, A. Zhugayevych, H. Shin, Y. S. Park, B. Kim, H. J. Yen, P. Cheruku, J. S. Martinez, J. W. Park, S. Tretiak and H. L. Wang, *Chemical Science*, 2015, **6**, 789-797.
3. OECD Screening Information Data Set (SIDS) program, <http://www.inchem.org>.
4. S. van Bezouw, J. Campo, S. H. Lee, O. P. Kwon and W. Wenseleers, *J. Phys. Chem. C*, 2015, **119**, 21658-21663; S. T. Abdelhalim, M. H. Abdelkader and U. E. Steiner, *J. Phys. Chem.*, 1988, **92**, 4324-4328; M. R. Mahmoud, R. Abdelhamide and K. A. Idriss, *Bull. Chem. Soc. Jpn.*, 1979, **52**, 574-578; H. W. Gibson and F. C. Bailey, *Can. J. Chem.-Rev. Can. Chim.*, 1975, **53**, 2162-2170; D. Prukala, W. Prukala, M. Gierszewski, J. Karolczak, I. Khmelinskii and M. Sikorski, *Dyes Pigment.*, 2014, **108**, 126-139.
5. J. Campo, F. Desmet, W. Wenseleers and E. Goovaerts, *Optics Express*, 2009, **17**, 4587-4604.
6. J. Campo, W. Wenseleers, J. M. Hales, N. S. Makarov and J. W. Perry, *J. Phys. Chem. Lett.*, 2012, **3**, 2248-2252.
7. P. Kaatz, E. A. Donley and D. P. Shelton, *J. Chem. Phys.*, 1998, **108**, 849-856.
8. D. R. Lide, *CRC Handbook of Chemistry and Physics*, 88th edition, CRC Press Taylor&Francis, 2007-2008.
9. C. Reichardt, *Chem. Rev.*, 1994, **94**, 2319-2358; C. Reichardt and T. Welton, *Solvents and Solvent Effects in Organic Chemistry*, Wiley-VCH Verlag, Weinheim, 4th edn., 2011.